

This article was downloaded by: [Siauliu University Library]

On: 17 February 2013, At: 00:39

Publisher: Taylor & Francis

Informa Ltd Registered in England and Wales Registered Number: 1072954 Registered office: Mortimer House, 37-41 Mortimer Street, London W1T 3JH, UK



## Molecular Crystals and Liquid Crystals

Publication details, including instructions for authors and subscription information:

<http://www.tandfonline.com/loi/gmcl20>

### Effect of Polymeric p-Type Semiconductor on Photovoltaic Properties in Dye-Sensitized Solar Cell

Kenji Yamada <sup>a</sup>, Yoshihisa Hayakawa <sup>a</sup>, Takeshi Okada <sup>a</sup>, Kazuya Yamamoto <sup>a</sup>, Tatsuhiko Sonoda <sup>a</sup>, Hiroyuki Nakamura <sup>a</sup> & Hirokazu Yamane <sup>a</sup>

<sup>a</sup> Department of Materials Science and Chemical Engineering, Kitakyushu National College of Technology, Shii, Kokuraminami-ku, Kitakyushu, Japan

Version of record first published: 17 Sep 2012.

To cite this article: Kenji Yamada , Yoshihisa Hayakawa , Takeshi Okada , Kazuya Yamamoto , Tatsuhiko Sonoda , Hiroyuki Nakamura & Hirokazu Yamane (2012): Effect of Polymeric p-Type Semiconductor on Photovoltaic Properties in Dye-Sensitized Solar Cell, Molecular Crystals and Liquid Crystals, 567:1, 1-8

To link to this article: <http://dx.doi.org/10.1080/15421406.2012.702373>

PLEASE SCROLL DOWN FOR ARTICLE

Full terms and conditions of use: <http://www.tandfonline.com/page/terms-and-conditions>

This article may be used for research, teaching, and private study purposes. Any substantial or systematic reproduction, redistribution, reselling, loan, sub-licensing, systematic supply, or distribution in any form to anyone is expressly forbidden.

The publisher does not give any warranty express or implied or make any representation that the contents will be complete or accurate or up to date. The accuracy of any instructions, formulae, and drug doses should be independently verified with primary sources. The publisher shall not be liable for any loss, actions, claims, proceedings, demand, or costs or damages whatsoever or howsoever caused arising directly or indirectly in connection with or arising out of the use of this material.

# Effect of Polymeric p-Type Semiconductor on Photovoltaic Properties in Dye-Sensitized Solar Cell

KENJI YAMADA,\* YOSHIHISA HAYAKAWA, TAKESHI OKADA, KAZUYA YAMAMOTO, TATSUHIKO SONODA, HIROYUKI NAKAMURA, AND HIROKAZU YAMANE

Department of Materials Science and Chemical Engineering, Kitakyushu National College of Technology, Shii, Kokuraminami-ku, Kitakyushu, Japan

*A hole formed in photo-excited dye molecule under illumination is transferred to cathode with iodine ion in electrolyte solution in the dye-sensitized solar cell developed by M. Grätzel and the conductivity of the iodine ion affects conversion efficiency of the cell. In this work, effect of the polymeric p-type semiconductor on the hole transferability is investigated. PEDOT:PSS and P3HT were used as the p-type semiconductors. Dye-sensitized solar cells were composed of aluminium plate, Nb-doped TiO<sub>2</sub> layer adsorbed with TCNQ, the electrolyte solution containing iodine ions, and ITO glass plate. In a solid-type cell substituted the electrolyte solution with the p-type semiconductor, photocurrent was not generated. The photocurrent was generated in the solar cell by introducing the electrolyte solution containing iodine ions between the ITO glass and the p-type semiconductor formed on the dye-adsorbed Nb-doped-TiO<sub>2</sub> layer or between the dye-adsorbed Nb-doped-TiO<sub>2</sub> layer and the p-type semiconductor formed on the ITO glass. The conversion efficiency increased with the introduction of the p-type semiconductor such as PEDOT:PSS, compared only with the electrolyte solution. The p-type semiconductor containing iodine ions promote the hole transfer of iodine ion, compared with that in the electrolyte solution.*

**Keywords** p-type semiconductor; titanium dioxide; dye; iodine; solar cell

## 1. Introduction

Conversion efficiency in a dye-sensitized solar cell (DSC) will be affected by the transportation property of a hole formed in photo-excited dye adsorbed on TiO<sub>2</sub> electrode. An I<sup>−</sup>/I<sub>3</sub><sup>−</sup> redox couple is played an important role for charge transport in DSC [1–3]. It was reported that both physical diffusion ( $D_{\text{phys}}$ ) and exchange-reaction based diffusion ( $D_{\text{ex}}$ ) of an I<sup>−</sup>/I<sub>3</sub><sup>−</sup> redox couple contribute to electron transport process in 1-ethyl-3-methylimidazolium bis(trifluoromethane sulfonyl)imide (EMImTFSI) and  $D_{\text{ex}}$  dominates over the whole charge transport processes at high I<sup>−</sup>/I<sub>3</sub><sup>−</sup> redox couple concentration [4–5]. The characteristic charge transport based on the exchange reaction of the I<sup>−</sup>/I<sub>3</sub><sup>−</sup> redox couple was revealed to occur only in the ionic liquid, although the physical diffusion of the redox couple in EMImTFSI and polyethylene glycol dimethylether (PEGDE) was similar

---

\*Address correspondence to Kenji Yamada, Department of Materials Science and Chemical Engineering, Kitakyushu National College of Technology, 5-20-1, Shii, Kokuraminami-ku, Kitakyushu 802-0985, Japan. Tel.: (+)-81-93-964-7305; Fax: (+)-81-93-964-7305. E-mail: kyamada@kct.ac.jp

[6]. Quasi-solid dye-sensitized solar cells (QDSC) were fabricated using the gel electrolyte which consisted of ionic liquids and nanoparticles modified with imidazolium cations [7]. The gel electrolyte looked like hard clay. However, the photocurrents of DSC consisting of the gels were almost same as those consisting of ionic liquid electrolyte. The ionic paths fabricated by ordered structures of imidazolium cations would assist the diffusions of  $I^-$  and  $I_3^-$  species [7].

Solid state dye-sensitized solar cell were fabricated using Ru-dye-sensitized nanoporous  $TiO_2$  electrode and conjugated polymer as hole transport materials [8]. The overall energy conversion efficiency of the solid state cell was more than one order of magnitude lower in efficiency compared to cells where an electrolyte solution is responsible for hole transport. The major problems associated with solid state cells seem to be the imperfect topological filling of a polymeric hole conductor into the pores between the nanoparticles together with the adhesion of the polymer on the  $TiO_2$  or on the Ru-dye [8].

In this work, effect of polymeric p-type semiconductors on the hole transferability is investigated in dye-sensitized solar cell. The transport of an  $I^-/I_3^-$  redox couple in the p-type semiconductors is also investigated.

## 2. Experimental Methods

### 2.1 Synthesis of Nb-Doped $TiO_2$

Nb-doped  $TiO_2$  particles were synthesized by means of metal alkoxide method. Titanium (IV) isopropoxide and niobium (V) ethoxide were used as the alkoxides. A mixture of the alkoxides and acetylacetone in which mole ratio was 1/1 was stirred at 313 K for 24 h and then at 353 K for 169 h to synthesize Nb-doped  $TiO_2$  sol. The mole ratio of niobium (V) ethoxide and titanium (IV) isopropoxide were 2/98 to 8/92, depending on Nb-doping amount in the particles.

### 2.2 Structural Analyses of Nb-Doped $TiO_2$

An UV-vis diffuse reflectance spectrum of the Nb-doped  $TiO_2$  particles was measured with a JASCO V-500 UV-vis spectrophotometer (JASCO International Co., Tokyo, Japan) equipped with an integral-sphere attachment to determine a change in light absorbance with Nb-doping. X-ray diffraction intensity (XRD) curves of the Nb-doped  $TiO_2$  particles were measured with a Rigaku Rint 1200 x-ray diffractometer (Rigaku Denki Co., Tokyo, Japan) using  $Cu K\alpha$  radiation with a generator voltage of 40 kV and tube current of 30 mA. After the instrumental broadening was corrected with a quartz standard, the full width at half maximum (FWHM) of the diffraction peak was evaluated for anatase (101) plane.

### 2.3 Preparation of Nb-Doped $TiO_2$ Electrodes and Evaluation of Their Flat Band Potentials

To prepare Nb-doped  $TiO_2$  paste, Nb-doped  $TiO_2$  particles were dispersed in 1M acetic acid solution to obtain a Nb-doped  $TiO_2$  concentration of 7 wt% and then mixed with polyethylene glycol (PEG) with a weight-average molecular weight of 3,000,000 to 3,500,000 under ultrasonic agitation to obtain a PEG/Nb-doped- $TiO_2$  weight ratio of 2/5. A thin film of the paste was coated on an aluminium plate using a screen-printing technique. The Nb-doped  $TiO_2$  film was sintered in air at 723 K for 30 min and then cooled to room temperature. The process of printing and sintering was repeated four times to prepare Nb-doped  $TiO_2$  electrode.

The capacitances of the space charge layer in the Nb-doped  $\text{TiO}_2$  electrodes were measured in 0.1 M  $\text{Na}_2\text{B}_4\text{O}_7$  solution of pH 7 at an alternating voltage of 10 mV and a frequency of 1 kHz with a NF LI5640 digital lock-in amplifier (NF Co., Yokohama, Japan). The temperature of the solution was 293 K. An Ag/AgCl electrode and platinum electrode were used as a reference electrode and a counter electrode, respectively. To evaluate the capacitance of the space charge layer as a function of electrode potential, the potential was changed from  $-1.0$  to  $+1.0$  V vs. Ag/AgCl with a Hokuto Denko HA-301 potentiostat (Hokuto Denko Co., Tokyo, Japan). The flat band potentials of the electrodes were evaluated using Mott-Schottky formula [9] and the capacitance of the space charge layer and electrode potential.

## 2.4 Fixation of Dye Molecules to the Nb-Doped $\text{TiO}_2$ Electrode

The Nb-doped  $\text{TiO}_2$  electrodes were immersed for two days in an acetonitrile solution containing 0.3 mM 7, 7, 8, 8-tetracyanoquinodimethane (TCNQ). The electrodes were then rinsed with acetonitrile and dried in a vacuum at room temperature.

## 2.5 Solar Cell Assembly

Figure 1 shows composition of solar cells I through IV fabricated in this work, as follows.

(1) *Solar cell I.* The electrolyte solution for the solar cell was composed of 40 mM iodine, 500 mM lithium iodide, and 580 mM 4-tert-butylpyridine (TBP) dissolved in acetonitrile (all the chemicals were purchased from Wako Pure Chemical Industries, Ltd., Osaka, Japan). To assemble the solar cell, the electrolyte solution was inserted between ITO glass plate as a cathode and the Nb-doped  $\text{TiO}_2$  electrode adsorbed with the dye as an anode. Sheet resistance of the ITO glass plate was  $5 \Omega$  per square.

(2) *Solar cell II.* Poly(3,4-ethylenedioxythiophene)-poly(styrenesulfonate) (PEDOT:PSS) was used as the p-type semiconductor. PEDOT:PSS solution in concentration 2.8 wt% in water was spin-coated on a surface of an anode, that is, the Nb-doped  $\text{TiO}_2$  electrode adsorbed with the dye and then dried in vacuum at 383 K for 30 min. Spin speed and time were 3000 r.p.m. and 30 s, respectively. The ITO glass plate was connected on the surface of PEDOT:PSS layer formed on the anode to assemble a solar cell (solar cell II).

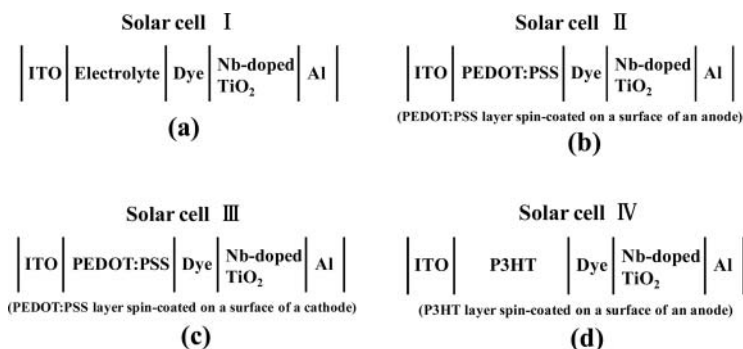


**Figure 1.** Composition of (a) solar cell I, (b) cell II, (c) cell III, and (d) cell IV, fabricated in this work.

X-ray photoelectron spectroscopy (XPS) measurement of the anode coated with PEDOT:PSS was carried out with a Shimadzu ESCA3400 x-ray photoelectron spectrometer (Shimadzu Co., Kyoto, Japan) to determine a change in surface structure with spin-coating. XPS spectra were collected by exciting the anode without pre-treatment with a Mg  $K_{\alpha}$  x-ray source. Mg  $K_{\alpha}$  radiation was generated with a voltage of 8 kV and current of 30 mA. The spectrometer was calibrated using the Ag $3d_{5/2}$  core line.

(3) *Solar cell III.* The PEDOT:PSS solution was spin-coated on a surface of a cathode, that is, the ITO glass plate and then dried in vacuum at 383 K for 30 min. Spin speed and time were 3000 r.p.m. and 30 s, respectively. The Nb-doped  $TiO_2$  electrode adsorbed with the dye was connected on the surface of PEDOT:PSS layer formed on the ITO glass plate to assemble a solar cell (solar cell III).

(4) *Solar cell IV.* Poly (3-hexylthiophene-2,5-diyl) (P3HT) instead of PEDOT:PSS was used as the p-type semiconductor. P3HT solution in concentration 1 wt% in chlorobenzene was spin-coated on a surface of the anode and then dried in vacuum at 313 K for 30 min, similar to the solar cell II. The ITO glass plate was connected on the surface of P3HT layer formed on the anode to assemble a solar cell (solar cell IV).

## 2.5 Characterization Analyses of Solar Cells

Photovoltaic properties of the solar cells were characterized by current-voltage characteristics under illumination with AM 1.5G simulated solar light with  $100 \text{ mWcm}^{-2}$  using a Peccell solar simulator PEC-L11 (Peccell Technologies Co., Kanagawa, Japan).

## 3. Results and Discussion

### 3.1. Characterization of Nb-Doped $TiO_2$

Figure 2 shows XRD curves of  $TiO_2$  and Nb-doped  $TiO_2$  particles after sintering in air at 723 K for 30 min. The type of the crystal structure was anatase in the  $TiO_2$  and the Nb-doped  $TiO_2$  particles and other crystal structure was not formed by Nb-doping. Such an anatase type crystal structure was not changed in the Nb-doped particles which were prepared

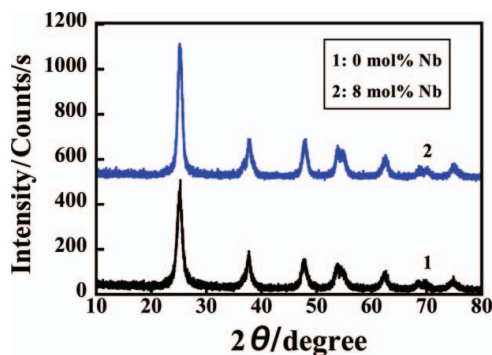


**Figure 2.** XRD curves of  $TiO_2$  and Nb-doped  $TiO_2$  particles after sintering in air at 723 K for 30 min. The Nb-doped  $TiO_2$  particles were prepared with mole ratio of niobium(V) ethoxide/ titanium(IV) isopropoxide equal to 8/92.

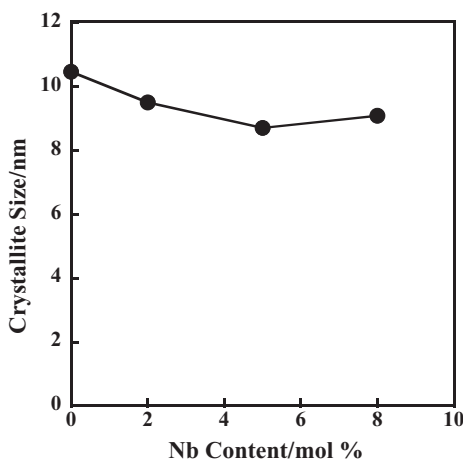


**Figure 3.** Size of anatase crystallites as a function of Nb content in the Nb-doped  $\text{TiO}_2$  particles after sintering in air at 723 K for 30 min.

below 8 mol % of niobium (V) ethoxide. Figure 3 shows the size of anatase crystallite as a function of Nb content in the Nb-doped  $\text{TiO}_2$  particles after sintering in air at 723 K for 30 min. The size of anatase crystallite is evaluated with Scherrer's equation, using the FWHM of the anatase (101) peak. The crystallite size was decreased with increasing Nb content. It is considered from Figures 2 and 3 that Nb atoms are homogeneously dispersed in the anatase crystallites.

Figure 4 shows UV-vis diffuse reflectance spectra of the Nb-doped  $\text{TiO}_2$  particles after sintering in air at 723 K for 30 min. Visible light absorption around 400 through 430 nm appeared in the Nb-doped  $\text{TiO}_2$  particles. Figure 5 shows flat band potential as a function of Nb content in the Nb-doped  $\text{TiO}_2$  electrodes below 8 mol% of Nb content. The electrodes were sintered in air at 723 K for 30 min. The flat band potential was decreased with

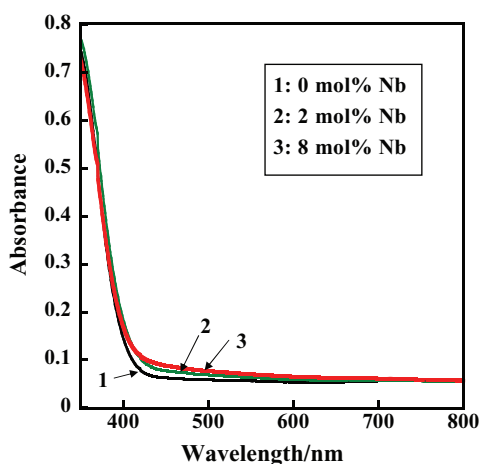


**Figure 4.** UV-vis diffuse reflectance spectra of the Nb-doped  $\text{TiO}_2$  particles after sintering in air at 723 K for 30 min.

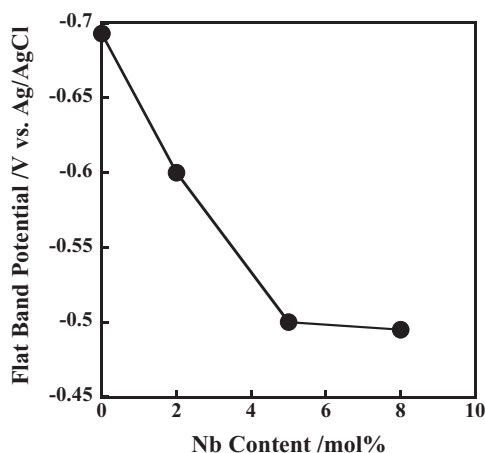


**Figure 5.** Flat band potential as a function of Nb content in the Nb-doped  $\text{TiO}_2$  electrodes after sintering in air at 723 K for 30 min.

increasing Nb content and therefore the lowest level of conduction band of the Nb-doped  $\text{TiO}_2$  electrode is positively shifted with increasing Nb content. A decrease in the flat band potential attains ca. 0.20 V at 8 mol% of Nb content. The visible-light absorption of the Nb-doped  $\text{TiO}_2$  particles shown in Figure 4 will be caused by the positive shift of the lowest level of the conduction band.

### 3.2 Effects of PEDOT:PSS

Figure 6 shows energy-level diagram of the solar cell I composed of aluminium plate, Nb-doped  $\text{TiO}_2$  electrode adsorbed with TCNQ, the electrolyte solution containing iodine ions, and ITO glass plate, as shown in Figure 1(a). In the solar cell I short-circuit current density  $J_{\text{sc}}$ , open-circuit voltage  $V_{\text{oc}}$ , and conversion efficiency  $\eta$  were  $0.14 \text{ mAcm}^{-2}$ , 0.55 V, and 0.03%, respectively. Therefore an electron photo-excited from HOMO of the dye to the conduction band of Nb-doped  $\text{TiO}_2$  is transferred to aluminium plate, whereas a hole remained in HOMO of the dye oxidizes  $\text{I}^-$  to form  $\text{I}_3^-$  in the electrolyte solution. The

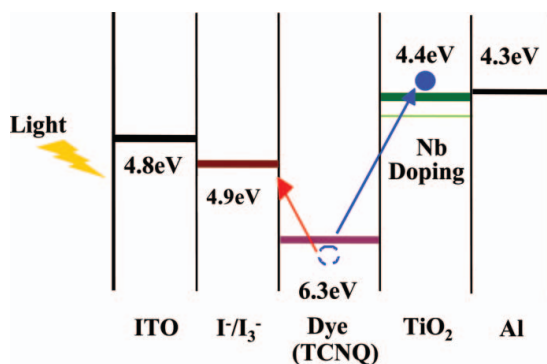


**Figure 6.** Energy-level diagram of solar cell I composed of aluminium plate, Nb-doped  $\text{TiO}_2$  electrode adsorbed with TCNQ, the electrolyte solution containing iodine ions, and ITO glass plate.

electron in aluminium plate is transferred to the ITO glass plate through outer circuit and then reduces  $I_3^-$  to  $I^-$  on the surface of the ITO glass plate.

In the solar cell II shown in Figure 1(b), photocurrent was not generated. Since the photo-excited electron in the dye can be transferred to aluminium plate, as shown in Figure 6, it is considered that a hole generated in the photo-excited dye can not transfer to ITO glass plate. Therefore a hole remained in HOMO of the photo-excited dye can not transfer to the valence band of PEDOT:PSS or the hole transferred to the valence band of PEDOT:PSS can not transfer to the ITO glass plate. Considering that the PEDOT:PSS layer and the ITO glass plate are mechanically contacted and the highest level of the valence band of the PEDOT:PSS layer is 5.0 eV [10], it is assumed that hole remained in HOMO of the photo-excited dye can transfer to the valence band of PEDOT:PSS, but the hole transferred to the valence band of PEDOT:PSS can not transfer to the ITO glass plate. When the electrolyte solution was inserted between the ITO glass plate and the PEDOT:PSS layer of the anode in the solar cell II, photocurrent was generated. In the solar cell II containing the electrolyte solution,  $J_{sc}$ ,  $V_{oc}$ , and  $\eta$  were  $0.49 \text{ mAcm}^{-2}$ , 0.55 V, and 0.08%, respectively. Conversion efficiency in the solar cell II containing the electrolyte solution was higher than that in the solar cell I. According to XPS spectra of the Nb-doped  $TiO_2$  electrode adsorbed with the dye and then covered with PEDOT:PSS layer,  $Ti_{2p}$  peak did not appear and  $S_{2p}$  peak did. Therefore it is confirmed that the thickness of the PEDOT:PSS layer is above a few nm. A hole in the HOMO of the photo-excited dye can oxidize  $I^-$  ion to form  $I_3^-$  ion, whereas  $I_3^-$  ion can not oxidize PEDOT:PSS, since  $I^-/I_3^-$  redox potential is 4.9 eV [11, 12] and higher than the highest level of the valence band of PEDOT:PSS. Therefore  $I_3^-$  ion will be diffused through the PEDOT:PSS layer and then reduced on the surface of ITO glass plate. It is considered for the increase in the conversion efficiency in the solar cell II containing the electrolyte solution that the rate of the diffusion of  $I_3^-$  through the PEDOT:PSS layer will be higher than that in the electrolyte solution.

In the solar cell III shown in Figure 1(c), photocurrent was not generated. It is considered that a hole remained in HOMO of the photo-excited dye can not transfer to the valence band of the PEDOT:PSS layer formed on the ITO glass plate, since the dye layer and the PEDOT:PSS layer are mechanically contacted. When the electrolyte solution was inserted between the PEDOT:PSS layer and Nb-doped  $TiO_2$  electrode adsorbed with the dye in the solar cell III, photocurrent was generated. In the solar cell III containing the electrolyte solution,  $J_{sc}$ ,  $V_{oc}$ , and  $\eta$  were  $0.62 \text{ mAcm}^{-2}$ , 0.64 V, and 0.17%, respectively. Conversion efficiency in the solar cell III containing the electrolyte solution was higher than that of the solar cell I. It is confirmed that  $I_3^-$  ion is diffused in the PEDOT:PSS layer and then reduced on the surface of ITO glass plate. An electron transferred from outer circuit can be transferred to the valence band of the PEDOT:PSS layer through the ITO glass plate, but  $I_3^-$  ion can not be reduced with the electron in valence band of the PEDOT:PSS layer, since  $I^-/I_3^-$  redox potential is higher than the highest level of the valence band of the PEDOT:PSS layer.

### 3.3 Effects of P3HT

In the solar cell IV shown in Figure 1(d), photocurrent was not generated. It is considered that a hole remained in HOMO of the photo-excited dye can not transfer to the valence band of P3HT or the hole transferred to the valence band of P3HT can not transfer to the ITO glass plate. Considering that the P3HT layer and the ITO glass plate are mechanically contacted and the highest level of the valence band of the P3HT layer is 5.1 eV [10], it is assumed that hole remained in HOMO of the photo-excited dye can transfer to the valence

band of P3HT, but the hole transferred to the valence band of P3HT can not transfer to the ITO glass plate. When the electrolyte solution was inserted between the ITO glass plate and the P3HT layer in the solar cell IV, photocurrent was generated. In the solar cell IV containing the electrolyte solution,  $J_{sc}$ ,  $V_{oc}$ , and  $\eta$  were  $0.11 \text{ mAcm}^{-2}$ ,  $0.52 \text{ V}$ , and  $0.02\%$ , respectively. Conversion efficiency in the solar cell IV containing the electrolyte solution was lower than that of the solar cell I. According to XPS spectra of the Nb-doped  $\text{TiO}_2$  electrode adsorbed with the dye and then covered with P3HT layer,  $\text{Ti}_{2p}$  peak did not appear and  $\text{S}_{2p}$  peak did. Therefore it is confirmed that the thickness of the P3HT layer is above a few nm. A hole in the HOMO of the dye can oxidize  $\text{I}^-$  ion to form  $\text{I}_3^-$  ion, whereas  $\text{I}_3^-$  ion can not oxidize P3HT, since  $\text{I}^-/\text{I}_3^-$  redox potential is higher than the highest level of the valence band of P3HT. Therefore  $\text{I}_3^-$  ion will be diffused in P3HT layer and then reduced on the surface of ITO glass plate.

#### 4. Conclusion

Nb atoms in the Nb-doped  $\text{TiO}_2$  are homogeneously dispersed into the anatase structure of  $\text{TiO}_2$  and the size of anatase crystallites evaluated with the FWHM of the anatase (101) plane is decreased with increasing Nb content below 8 mol%. The flat band potential in the Nb-doped  $\text{TiO}_2$  is decreased with increasing Nb content. A decrease in the flat band potential attains ca.  $0.20 \text{ V}$  at 8 mol% of Nb content.

The photocurrent is generated in the solar cell II, III, and IV containing the electrolyte solution. When the PEDOT:PSS layer is formed on the surface of the Nb-doped electrode adsorbed with the dye or on the surface of the ITO glass plate,  $\text{I}^-/\text{I}_3^-$  ions will be diffused in the PEDOT:PSS layer and the rate of diffusion of  $\text{I}^-/\text{I}_3^-$  ions in the PEDOT:PSS layer will be higher than that in the electrolyte solution.

#### References

- [1] Grätzel, M. (2001). *Nature*, *414*, 338.
- [2] Grätzel, M. (2003). *J. Photochem. Photobiol. C*, *4*, 145.
- [3] Grätzel, M. (2005). *Chem. Lett.*, *34*, 8.
- [4] Kawano, R., & Watanabe, M. (2003). *Chem. Commun.* 330.
- [5] Yamanaka, N., Kawano, R., Kubo, W., Kitamura, T., Wada, Y., Watanabe, M., & Yanagida, S. (2005). *Chem. Commun.* 740.
- [6] Kawano, R., & Watanabe, M. (2005). *Chem. Commun.* 2107.
- [7] Kato, T., Kado, T., Tanaka, S., Okazaki, A., & Hayase, S. (2006). *J. Electrochem. Soc.*, *153*, A626.
- [8] Gebeyehu, D., Brabec, C. J., Sariciftci, N. S., Vangeneugden, D., Kiebooms, R., Vanderzande, D., Kienberger, F., & Schindler, H. (2002). *Synth. Met.*, *125*, 279.
- [9] van der Krol, R., Goossens, A., & Schoonman, J. (1997). *J. Electrochem. Soc.*, *144*, 1723.
- [10] Kim, J. Y., Lee, K., Coates, N. E., Moses, D., Nguyen, T. Q., Dante, M., & Heeger, A. J. (2007). *Science*, *317*, 222.
- [11] O'Regan, B., & Grätzel, M. (1991). *Nature*, *353*, 737.
- [12] Barbe, C. J., Arendse, F., Comte, P., Jirousek, M., Lenzman, F., Shklover, V., & Grätzel, M. (1997). *J. Am. Ceram. Soc.*, *80*, 3157.